

Spin-orbit splitting of organic cavity polaritons and its effect on superradiant transition

Shoaib Masood, Hamdan Tariq, and M. Ahsan Zeb

Department of Physics, Quaid-i-Azam University, Islamabad 45320, Pakistan

(Dated: 05/01/2021)

Using an extended Dicke model, we study the effect of the spin-orbit coupling between the singlet and the triplet molecular excitons in organic microcavities. We exactly solve the model in the strong coupling regime in the single excitation space. We calculate the polaritonic states and the optical absorption spectrum of the system and explore the spin-orbit induced splitting of the lower polariton into two branches. The effect of this splitting in the ultra strong coupling regime on the superradiant phase transition is explored using a variational approach. We find that the spin-orbit coupling pushes the system towards the superradiant phase and reduces the critical matter-light coupling required for it.

I. INTRODUCTION

The role of the strong matter-light coupling [1–5] in modifying and determining various physical properties is extensively studied over the past two decades. Some important examples include the formation of polariton condensates [6–18], effect on superconducting phases [19–24], charge and energy transport [25–32], and chemical reaction rates [33–42]. Organic microcavities form an important class of systems that exhibit the strong matter-light coupling where the presence of the intramolecular vibrations and the triplet molecular excitons significantly enriches the prospects [1–18, 33–42]. The vibronic coupling and polaronic effects in these systems are very important and usually included in the models [32, 43]. However, the spin-orbit coupling between the singlet molecular exciton and the triplet molecular excitons in organic microcavities is gaining attention only very recently [44]. Since the cavity modes couple only to the singlet molecular excitons, the spin-orbit coupling between the singlet and the triplet can indirectly couple the latter to the cavity mode. Compared to the singlet excitons or polaritons, the electronic pumping of organic microcavities creates three times as many triplets and it is desired to make them emissive or use them to increase the polariton population for condensation or lasing.

The triplet excitons in organic molecules lie below the singlet excitons (by the exchange splitting $J \sim 0.5 - 1$ eV) and thermally activated processes (the reverse inter-system crossing, RISC) cannot do much. Fortunately, the strength of the matter-light coupling in organic microcavities that is experimentally achievable has increased over the time and recently it was demonstrated to even bring the lower polariton (LP) below the triplet exciton state, the so called inverted regime [45]. But, the density of the “dark” singlet and triplet excitons being dominating still keeps the molecular excitations from the light emission [45, 46]. Does this mean there is nothing important the spin-orbit can do in these systems? Here, we explore the effect of the spin-orbit coupling on the polaritonic states of organic microcavities using an extended Dicke model [47]. As shown in

Fig. 1, the LP originating from the coupling ω_R between the singlet exciton and the cavity mode can be made resonant to the triplet excitons as ω_R approaches J . In such a case, the effect of the spin-orbit coupling between the singlet exciton component in the LP and the triplet becomes significant. Using the exact numerics, we find that it splits the LP into two branches LP_{\pm} that can be seen in the optical absorption spectrum. Further, employing a variational method, we show that this spin-orbit splitting drives the system towards its superradiant phase [48, 49].

We describe the model and a useful unitary transformation to simplify it in sec. II. Section III contains the exact numerical results for the polaritonic states and optical absorption spectrum. We present an approximate analytical solution for the two spin-orbit split branches LP_{\pm} in sec. IV. The effect of the spin-orbit coupling on the superradiant phase transition is discussed in sec. V.

II. MODEL

Consider N identical conjugated organic molecules placed inside a microcavity formed by, say, two plane mirrors with a separation that is of the order of half the wavelength that excites a singlet exciton on the organic molecules. This hybrid system couples the matter excitations to the cavity photons and can be excited optically or electronically. We assume that only a single cavity mode couples to the molecules and the system is in the strong coupling regime, i.e., the matter-light coupling is larger than the losses, the cavity leakage and the non-radiative exciton decay. For simplicity, we consider three electronic states of a molecule: $|G\rangle, |S\rangle, |T\rangle$ — ground, singlet and triplet state. In this state space of a molecule i , the creation and annihilation operators for the singlet ($\hat{\sigma}_i^{\pm}$) and triple ($\hat{\tau}_i^{\pm}$) excitons can be defined as

$$\hat{\sigma}_i^{\pm} = \begin{pmatrix} 0 & 0 & 0 \\ 1 & 0 & 0 \\ 0 & 0 & 0 \end{pmatrix}, \quad \hat{\tau}_i^{\pm} = \begin{pmatrix} 0 & 0 & 0 \\ 0 & 0 & 0 \\ 1 & 0 & 0 \end{pmatrix},$$

$$\hat{\sigma}_i^- = (\hat{\sigma}_i^+)^{\dagger}, \quad \hat{\tau}_i^- = (\hat{\tau}_i^+)^{\dagger}.$$

The Hamiltonian of N molecules coupled to a common

cavity mode can then be written as

$$\hat{\mathcal{H}} = \omega_c \hat{a}^\dagger \hat{a} + \sum_{i=1}^N \left\{ \omega_s \hat{\sigma}_i^+ \hat{\sigma}_i^- + \frac{\omega_R}{\sqrt{N}} (\hat{a}^\dagger + \hat{a})(\hat{\sigma}_i^+ + \hat{\sigma}_i^-) + [\omega_t \hat{\tau}_i^+ \hat{\tau}_i^- + \lambda(\hat{\sigma}_i^+ \hat{\tau}_i^- + \hat{\tau}_i^+ \hat{\sigma}_i^-)] \right\}, \quad (1)$$

where \hat{a}^\dagger, \hat{a} are the creation and annihilation operators for the cavity photons, ω_c , ω_s and ω_t are the energies of cavity mode, singlet exciton and triplet exciton. ω_R is the matter-light coupling whereas λ is the spin-orbit coupling between singlet and triplet exciton states. If we consider all three triplets, $|T\rangle$ would be a symmetric superposition of them, while the two non-symmetric superpositions would be decoupled. At $\lambda = 0$, the model reduces to the Dicke [47] or the Tavis-Cummings (TC) model [50] along with the decoupled triplet states. In the strong coupling regime [51, 52], we can use the rotating wave approximation [51], whereby Eq. 1 reduces to

$$\hat{\mathcal{H}}_{RWA} = \omega_c \hat{a}^\dagger \hat{a} + \sum_{i=1}^N \left\{ \omega_s \hat{\sigma}_i^+ \hat{\sigma}_i^- + \frac{\omega_R}{\sqrt{N}} (\hat{a}^\dagger \hat{\sigma}_i^- + \hat{\sigma}_i^+ \hat{a}) + [\omega_t \hat{\tau}_i^+ \hat{\tau}_i^- + \lambda(\hat{\sigma}_i^+ \hat{\tau}_i^- + \hat{\tau}_i^+ \hat{\sigma}_i^-)] \right\}. \quad (2)$$

$\hat{\mathcal{H}}_{RWA}$ commutes with the number of excitations \mathcal{N}_{ex} , where

$$\mathcal{N}_{ex} = \hat{a}^\dagger \hat{a} + \sum_i (\hat{\sigma}_i^+ \hat{\sigma}_i^- + \hat{\tau}_i^+ \hat{\tau}_i^-), \quad (3)$$

so we can diagonalise them simultaneously. Defining the Fourier transforms,

$$\hat{\mathcal{S}}_k^+ \equiv \frac{1}{\sqrt{N}} \sum_{j=1}^N e^{\frac{i2\pi kj}{N}} \hat{\sigma}_j^+ \quad (4)$$

$$\hat{\mathcal{T}}_k^+ \equiv \frac{1}{\sqrt{N}} \sum_{j=1}^N e^{\frac{i2\pi kj}{N}} \hat{\tau}_j^+, \quad (5)$$

we can simplify Eq. 2 to

$$\hat{\mathcal{H}}_{RWA} = \hat{\mathcal{H}}_B + \hat{\mathcal{H}}_D, \quad (6)$$

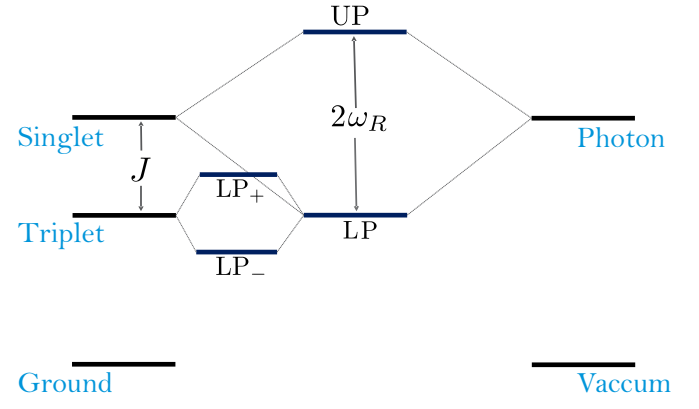
where

$$\begin{aligned} \hat{\mathcal{H}}_B &= \omega_c \hat{a}^\dagger \hat{a} + \omega_s \hat{\mathcal{S}}_0^+ \hat{\mathcal{S}}_0^- + \omega_t \hat{\mathcal{T}}_0^+ \hat{\mathcal{T}}_0^- \\ &\quad + \omega_R (\hat{a}^\dagger \hat{\mathcal{S}}_0^- + \hat{\mathcal{S}}_0^+ \hat{a}) + \lambda (\hat{\mathcal{T}}_0^+ \hat{\mathcal{S}}_0^- + \hat{\mathcal{S}}_0^+ \hat{\mathcal{T}}_0^-), \end{aligned} \quad (7)$$

$$\begin{aligned} \hat{\mathcal{H}}_D &= \sum_{k \neq 0} \omega_s \hat{\mathcal{S}}_k^+ \hat{\mathcal{S}}_k^- + \omega_t \hat{\mathcal{T}}_k^+ \hat{\mathcal{T}}_k^- \\ &\quad + \lambda (\hat{\mathcal{S}}_k^+ \hat{\mathcal{T}}_k^- + \hat{\mathcal{T}}_k^+ \hat{\mathcal{S}}_k^-), \end{aligned} \quad (8)$$

where there is no coupling between $\hat{\mathcal{H}}_B$ and $\hat{\mathcal{H}}_D$.

From hereon we will consider a single excitation, $\mathcal{N}_{ex} = 1$, until the very end where we solve Eq. 1 variationally for the superradiant phase transition. In the single excitation subspace, $\hat{\mathcal{H}}_D$ is a sum of 2-level-systems



Ground ————— Vacuum

FIG. 1: A sketch of the energy level diagram showing three molecular states considered (on the left) as well as the lowest two cavity states (on the right). The coupling between the singlet exciton and the cavity photon state creates the lower and the upper polaritons, LP and UP. Roughly speaking, the LP couples to the triplet molecular exciton state and produces LP_{\pm} .

so its diagonalisation is trivial. It is the “dark” sector of the spectrum. We are more interested in the “bright” sector represented by $\hat{\mathcal{H}}_B$. $\hat{\mathcal{H}}_B$ is a 3-level-system that can be numerically diagonalised. For experimentally relevant parameter regime $\omega_R, J \sim 0.5 - 1\text{eV}$, however, we can adiabatically eliminate the high energy state originating from the upper polariton (UP) to obtain an effective 2-level-system describing the low energy polaritonic branches of the spectrum. In the space of $|G\rangle \otimes |1_P\rangle, \hat{\mathcal{S}}_0^+ |G\rangle \otimes |0_P\rangle, \hat{\mathcal{T}}_0^+ |G\rangle \otimes |0_P\rangle$, where $|0_P\rangle$ and $|1_P\rangle$ are the cavity states with 0 and 1 photons, we can write

$$\hat{\mathcal{H}}_B = \begin{pmatrix} \omega_c & \omega_R & 0 \\ \omega_R & \omega_s & \lambda \\ 0 & \lambda & \omega_t \end{pmatrix} \equiv \begin{pmatrix} \delta & \omega_R & 0 \\ \omega_R & 0 & \lambda \\ 0 & \lambda & -J \end{pmatrix}, \quad (9)$$

where we define the detuning $\delta \equiv \omega_c - \omega_s$, exchange splitting $J \equiv \omega_s - \omega_t$, and set $\omega_s = 0$ as the reference.

III. NUMERICAL RESULTS

To explore the effects of the spin-orbit coupling in organic microcavities, the system Hamiltonian, Eq. 2, is solved numerically for different parametric regimes. The effect of the spin-orbit coupling is maximised when the singlet and the triplet states are brought closer in energy. For a given J , this occurs when the LP comes closer to the triplet, i.e., at $\omega_R \sim J$.

A. Lower polariton splitting

Figure 2(a) shows the spectrum of $\hat{\mathcal{H}}_B$, i.e., the energy of the polaritonic states of the system at $J = 0.5\text{eV}$,

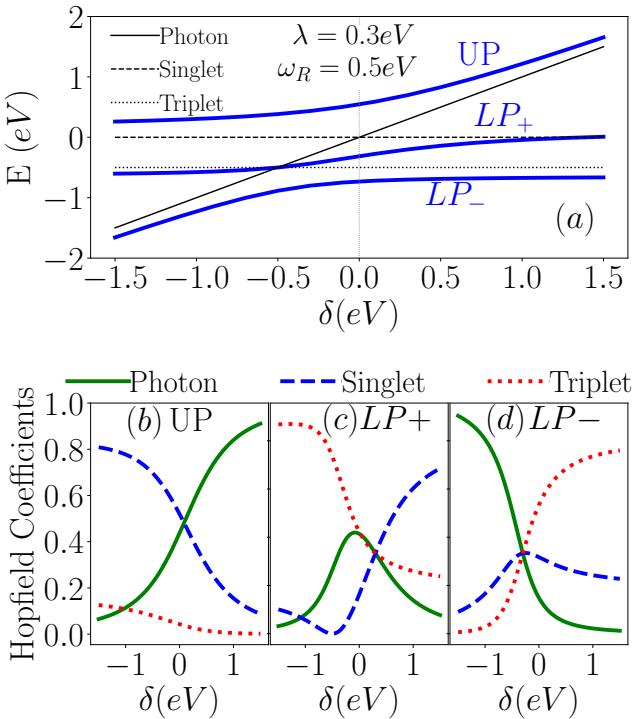


FIG. 2: The polaritonic states UP, LP_+ and LP_- at $\omega_R = 0.5$ eV, $\lambda = 0.3$ eV and $J = 0.5$ eV. (a) The energy of UP and LP_\pm along with the bare energies of the three components — the cavity photon and the molecular excitons. (b-d) The Hopfield coefficients, i.e., the weights of the component states.

$\omega_R = 0.5$ eV and $\lambda = 0.3$ eV. The energy of bare singlet, triplet and photon is also plotted. We call the highest energy state UP and the two lowest energy states LP_\pm , due to their relation to the upper and lower polaritons of Tavis-Cummings model (i.e., $\lambda = 0$ case). In Fig. (2)(a), two anti-crossings can be observed: one between UP and LP_+ near zero, the energy of the singlet state, and one between LP_\pm near the energy of the triplet state, $-J = -0.5$ eV. LP_\pm can be thought of as arising from the splitting of the LP due to its interaction with the triplet state, hence the names. Since all three states contain the photon component, the extra stabilisation of the lowest state due to this interaction has important consequences, as will be discussed later in sec. V.

B. Eigenstate structure

The three polaritonic states contain photon, singlet and triplet exciton state components. For a given eigenstate, we call the weights of these components its Hopfield coefficients. Figure 2(b-d) shows the Hopfield coefficients for the three eigenstates for the same parameters as in Fig. (2)(a). UP is far away from the triplet state so there is negligible triplet component in this branch, where as

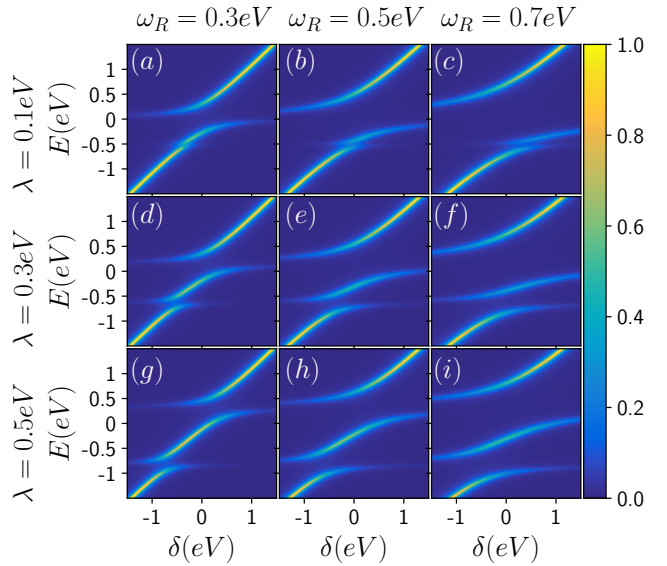


FIG. 3: Absorption spectrum at $J = 0.5$ eV. The matter-light coupling ω_R varies along the row where as the spin-orbit coupling λ changes along the column. At fixed ω_R (in a column), the lower polariton splits into two branches LP_\pm as we move to lower rows to increase λ . The effect becomes more prominent as we increase ω_R and bring the LP energy closer to that of the triplet exciton.

its singlet and photon components seem are only slightly affected by a finite spin-orbit coupling λ . Close to resonance ($\delta = 0$), all states have a non-zero photon component. LP_\pm both contain sizeable triplet component. LP_+ contains the photon only close to the resonance and it approaches to excitons away from it. The singlet component in LP_- decreases away from the resonance but it still stays relatively large. On the other hand this state approaches the photon or the triplet away from the resonance.

From the structure of LP_- , one can naively think that it might help the triplet to singlet transition that is highly desirable for optoelectronic devices. However, as Ref. [46] shows, the density of the dark triplet and singlet states, eigenstates of \hat{H}_D , is much larger and determine the reverse intersystem crossing rates. In other words, it is only the permutation symmetric superposition of the singlet and triplet that make up the polaritonic states. However, we find that this singlet-triplet mixing can still have significant effects, discussed in sec. V.

C. Absorption Spectrum

In experiments, measuring the optical absorption by the organic microcavities is a standard method to investigate the strong matter-light coupling and polaritons. In this section, we present the calculated absorption spec-

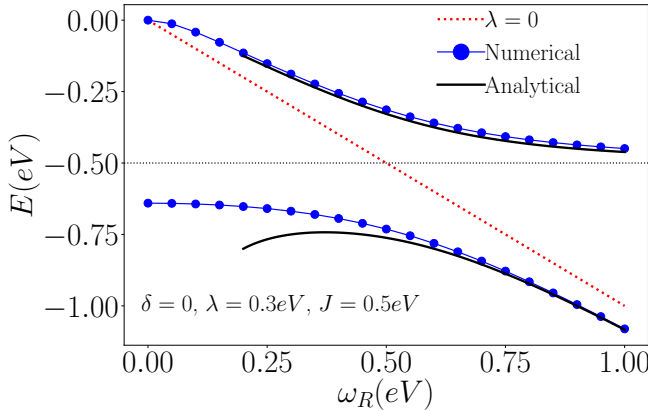


FIG. 4: The lower polariton splitting. Comparison of analytical and numerical results for the low energy eigenstates. The parameters used are $\delta = 0$, $\lambda = 0.3$ eV and $J = 0.5$ eV. The triplet energy $-J$ as well as the LP energy at $\lambda = 0$, i.e., $-\omega_R$, are also shown as dotted lines.

trum of our system for a select set ω_R and λ values. Figure 3 shows the absorption spectrum versus detuning δ at $J = 0.5$ eV. The value of ω_R varies from 0.3 eV to 0.7 eV along the row from the left to the right, and λ varies from 0.1 eV to 0.5 eV from the top to the bottom along the column. Starting from the top left, Fig. (3)(a), and moving to the right, we see very faint effect of the triplet and the absorption appears almost that of the singlet polaritons of the TC model. However, as we increase λ to 0.3 eV, move to the second row, the second anti-crossing now becomes prominent and we clearly see the splitting of the LP into two branches. The splitting increases as we increase ω_R because the decreased effective detuning between the singlet polariton and the triplet state. Increasing λ further to 0.5 eV in the bottom row, this splitting increases accordingly and in Fig. (3)(i), the two branches of the LP, LP_\pm even become deceptive — could be found in the experiments but look similar to the usual singlet polaritons. Looking at columns, from the top to the bottom, i.e., at fixed ω_R , we observe the LP splitting into LP_\pm as λ increases.

IV. ANALYTICAL RESULTS

At $\lambda = 0$, $\hat{\mathcal{H}}_B$ can be solved analytically, giving the two singlet exciton polaritons $|\pm\rangle$ of *Tavis–Cummings* model and the decoupled triplet exciton state. A unitary transformation to these basis states can indicate the origin of the LP splitting at $\lambda \neq 0$ and help us obtain an approximate analytical result for the two low energy branches, LP_\pm . Let's take the resonant case, $\delta = 0$, to

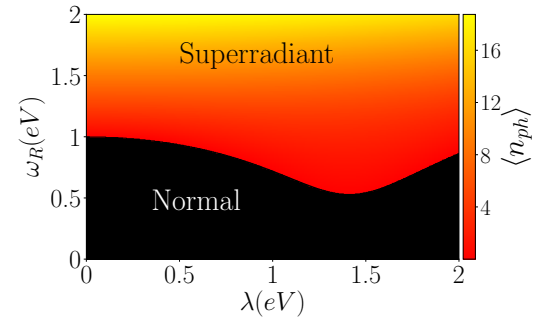


FIG. 5: Phase diagram in $\lambda - \omega_R$ space at $N = 20, \delta = 0, \omega_c = 2$ eV, $J = 1$ eV, $\beta = 10$ eV $^{-1}$. A finite λ can push the system to its superradiance phase by suppressing the required critical value of ω_R .

illustrate this point. $\hat{\mathcal{H}}_B$ can be written as

$$\hat{\mathcal{H}}_B = \begin{pmatrix} +\omega_R & 0 & \frac{\lambda}{\sqrt{2}} \\ 0 & -\omega_R & \frac{\lambda}{\sqrt{2}} \\ \frac{\lambda}{\sqrt{2}} & \frac{\lambda}{\sqrt{2}} & -J \end{pmatrix}, \quad (10)$$

which, on adiabatic elimination [53] of the UP (the high energy state at $+\omega_R$), reduces to

$$\hat{\mathcal{H}}_B = \begin{pmatrix} -\omega_R & \frac{\lambda}{\sqrt{2}} \\ \frac{\lambda}{\sqrt{2}} & -J - \frac{\lambda^2}{2\omega_R} \end{pmatrix}. \quad (11)$$

This reduced model of the two lower energy states is a good approximation in the parameter regime, $\omega_R \gtrsim J$.

$$\begin{aligned} E_\pm &= -\Delta \pm \sqrt{\Delta^2 - J\omega_R}, \\ \Delta &= (\omega_R + J)/2 + \lambda^2/4\omega_R. \end{aligned} \quad (12)$$

Figure 4 compares Eq. 12 and exact numerical low energy spectrum at $\delta = 0, \lambda = 0.3$ eV, $J = 0.5$ eV. The red dotted line shows the energy of the LP when there is no spin-orbit coupling, $\lambda = 0$. The analytical results agree reasonably well to the exact numerical results at $\omega_R \gtrsim J$.

V. SUPERRADIANCE

Since the splitting of the LP lowers the energy of the lowest polaritonic state, it is expected to push the system towards the superradiant phase in the ultra-strong coupling regime. We confirm this in the following using a variational method to calculate the ground state of the system[54].

A variational ansatz for the photon state $|\alpha\rangle$ in the superradiant phase can reduce the problem to electronic degrees of freedom only. Assuming,

$$|\alpha\rangle = e^{-|\alpha|^2/2} e^{\alpha a^\dagger} |0\rangle, \quad (13)$$

where $|0\rangle$ is the photon vacuum state, and $|\alpha|^2$ gives the average photon number $\langle n_{ph} \rangle$. Using this ansatz, we

can reduce the diagonalisation problem to the molecular states only. From the partition function $\mathcal{Z}_\alpha = \text{Tr}[e^{-\beta\hat{\mathcal{H}}_\alpha}]$, where $\hat{\mathcal{H}}_\alpha \equiv \langle \alpha | \hat{\mathcal{H}} | \alpha \rangle$ and β is the inverse temperature, the free energy $F_\alpha = -\frac{\partial}{\partial\beta} \log(\mathcal{Z}_\alpha)$ can be obtained. A minimum of F_α at $\alpha \neq 0$ would imply the superradiant phase, $\langle n_{ph} \rangle > 0$.

Figure 5 shows the phase diagram of the model in the space of λ and ω_R , at $N = 20$, $\delta = 0$, $\omega_c = 2\text{ eV}$, $J = 1\text{ eV}$, $\beta = 10\text{ eV}^{-1}$. The critical value of ω_R for the superradiant phase ($\langle n_{ph} \rangle > 0$) decreases as λ increases until $\lambda \sim 1.5\text{ eV}$ because the LP splitting increases that lowers the ground state energy just as we saw earlier in the single excitation space of \mathcal{H}_{RWA} . The experimentally realisable parameter regime $\lambda \lesssim \omega_R \sim 1\text{ eV}$ lies here so in real systems with large enough λ , e.g., organic materials containing heavy elements like Ir, the LP splitting could possibly push the system to the superradiant phase. The effect of spin-orbit coupling decreases at $\lambda \gtrsim 1.5\text{ eV}$ as the exciton character of the ground state increases sup-

pressing the photon component due to an effective detuning between the cavity states and the spin-orbit coupled exciton states.

VI. SUMMARY AND CONCLUSION

We investigate the role of the spin-orbit coupling between the singlet and the triplet molecular excitons in organic microcavities. We decouple the system into a bright sector that forms polaritons and a dark sector containing the dark exciton states that are decoupled from the cavity. The spin-orbit coupling splits the lower polariton into two branches that can be observed in the optical absorption spectrum. Using a variational method, we showed that the spin-orbit coupling can suppress the critical matter-light coupling required for the transition to the superradiant phase. Using exact numerics to study this phase transition as well as the role of the vibronic coupling in this system can be an interesting future work.

[1] D. G. Lidzey, D. Bradley, M. Skolnick, T. Virgili, S. Walker, and D. Whittaker, *Nature* **395**, 53 (1998).

[2] D. G. Lidzey, D. D. C. Bradley, T. Virgili, A. Armitage, M. S. Skolnick, and S. Walker, *Phys. Rev. Lett.* **82**, 3316 (1999).

[3] D. G. Lidzey, D. D. Bradley, A. Armitage, S. Walker, and M. S. Skolnick, *Science* **288**, 1620 (2000).

[4] R. J. Holmes and S. R. Forrest, *Phys. Rev. Lett.* **93**, 186404 (2004).

[5] J. R. Tischler, M. S. Bradley, V. Bulović, J. H. Song, and A. Nurmikko, *Phys. Rev. Lett.* **95**, 036401 (2005).

[6] J. Kasprzak, M. Richard, S. Kundermann, A. Baas, P. Jeambrun, J. M. J. Keeling, F. M. Marchetti, M. H. Szymańska, R. André, J. L. Staehli, V. Savona, P. B. Littlewood, B. Deveaud, and L. S. Dang, *Nature* **443**, 409 (2006).

[7] R. Balili, V. Hartwell, D. Snoke, L. Pfeiffer, and K. West, *Science* **316**, 1007 (2007).

[8] I. Carusotto and C. Ciuti, *Rev. Mod. Phys.* **85**, 299 (2013).

[9] S. Kéna-Cohen and S. R. Forrest, *Nat. Photonics* **4**, 371 (2010).

[10] K. S. Daskalakis, S. A. Maier, R. Murray, and S. Kéna-Cohen, *Nat. Mater.* **13**, 271 (2014).

[11] J. D. Plumhof, T. Stöferle, L. Mai, U. Scherf, and R. F. Mahrt, *Nat. Mater.* **13**, 247 (2013).

[12] R. T. Grant, P. Michetti, A. J. Musser, P. Gregoire, T. Virgili, E. Vella, M. Cavazzini, K. Georgiou, F. Galeotti, C. Clark, J. Clark, C. Silva, and D. G. Lidzey, *Adv. Opt. Mater.* **4**, 1615 (2016).

[13] T. Cookson, K. Georgiou, A. Zasedatelev, R. T. Grant, T. Virgili, M. Cavazzini, F. Galeotti, C. Clark, N. G. Berloff, D. G. Lidzey, and P. G. Lagoudakis, *Adv. Opt. Mater.* **5**, 1700203 (2017).

[14] C. P. Dietrich, A. Steude, L. Tropf, M. Schubert, N. M. Kronenberg, K. Ostermann, S. Höfling, and M. C. Gather, *Sci. Adv.* **2**, e1600666 (2016).

[15] S. Betzold, M. Dusel, O. Kyriienko, C. Dietrich, S. Klembt, J. Ohmer, U. Fischer, I. A. Shelykh, C. Schneider, and S. Höfling, *ACS Photonics* **7**, 384 (2019).

[16] S. K. Rajendran, M. Wei, H. Ohadi, A. Ruseckas, G. A. Turnbull, and I. D. W. Samuel, *Adv. Opt. Mater.* **7**, 1801791 (2019).

[17] M. Wei, S. K. Rajendran, H. Ohadi, L. Tropf, M. C. Gather, G. A. Turnbull, and I. D. W. Samuel, *Optica* **6**, 1124 (2019).

[18] J. Keeling and S. Kéna-Cohen, *Ann. Rev. Phys. Chem.* **71** (2020), 10.1146/annurev-physchem-010920-102509.

[19] M. A. Sentef, M. Ruggenthaler, and A. Rubio, *Sci. Adv.* **4** (2018), 10.1126/sciadv.aau6969.

[20] A. Thomas, E. Devaux, K. Nagarajan, T. Chervy, M. Seidel, D. Hagenmüller, S. Schütz, J. Schachenmayer, C. Genet, G. Pupillo, *et al.*, “Exploring superconductivity under strong coupling with the vacuum electromagnetic field,” (2019), preprint, 1911.01459.

[21] D. Fausti, R. I. Tobey, N. Dean, S. Kaiser, A. Dienst, M. C. Hoffmann, S. Pyon, T. Takayama, H. Takagi, and A. Cavalleri, *Science* **331**, 189 (2011).

[22] R. Mankowsky, A. Subedi, M. Först, S. O. Mariager, M. Chollet, H. T. Lemke, J. S. Robinson, J. M. Glowacka, M. P. Minitti, A. Frano, M. Fechner, N. A. Spaldin, T. Loew, B. Keimer, A. Georges, and A. Cavalleri, *Nature* **516**, 71 (2014).

[23] M. Mitrano, A. Cantaluppi, D. Nicoletti, S. Kaiser, A. Perucchi, S. Lupi, P. Di Pietro, D. Pontiroli, M. Riccò, S. R. Clark, D. Jaksch, and A. Cavalleri, *Nature* **530**, 461 (2016).

[24] F. Schlawin, A. S. D. Dietrich, M. Kiffner, A. Cavalleri, and D. Jaksch, *Phys. Rev. B* **96**, 064526 (2017).

[25] E. Orgiu, J. George, J. A. Hutchison, E. Devaux, J. F. Dayen, B. Doudin, F. Stellacci, C. Genet, J. Schachenmayer, C. Genes, G. Pupillo, P. Samorì, and T. W. Ebbesen, *Nat. Mater.* **14**, 1123 (2015).

[26] J. Feist and F. J. Garcia-Vidal, Phys. Rev. Lett. **114**, 196402 (2015).

[27] J. Schachenmayer, C. Genes, E. Tignone, and G. Pupillo, Phys. Rev. Lett. **114**, 196403 (2015).

[28] D. Hagenmüller, J. Schachenmayer, S. Schütz, C. Genes, and G. Pupillo, Phys. Rev. Lett. **119**, 223601 (2017).

[29] D. Hagenmüller, S. Schütz, J. Schachenmayer, C. Genes, and G. Pupillo, Phys. Rev. B **97**, 205303 (2018).

[30] C. Schäfer, M. Ruggenthaler, H. Appel, and A. Rubio, Proc. Natl. Acad. Sci. U. S. A. **116**, 4883 (2019).

[31] T. Botzung, D. Hagenmüller, S. Schütz, J. Dubail, G. Pupillo, and J. Schachenmayer, “Dark state localization of quantum emitters in a cavity,” (2020), preprint, 2003.07179.

[32] M. A. Zeb, P. G. Kirton, and J. Keeling, “Incoherent charge transport in an organic polariton condensate,” (2020), arXiv:2004.09790 [cond-mat.quant-gas].

[33] J. A. Hutchison, T. Schwartz, C. Genet, E. Devaux, and T. W. Ebbesen, Ang. Chem. Int. Ed. **51**, 1592 (2012).

[34] A. Thomas, J. George, A. Shalabney, M. Dryzhakov, S. J. Varma, J. Moran, T. Chervy, X. Zhong, E. Devaux, C. Genet, J. A. Hutchison, and T. W. Ebbesen, Ang. Chem. Int. Ed. **55**, 11462 (2016).

[35] A. Thomas, L. Lethuillier-Karl, K. Nagarajan, R. M. A. Vergauwe, J. George, T. Chervy, A. Shalabney, E. Devaux, C. Genet, J. Moran, and T. W. Ebbesen, Science **363**, 615 (2019).

[36] F. Herrera and F. C. Spano, Phys. Rev. Lett. **116**, 238301 (2016).

[37] J. Galego, F. J. Garcia-Vidal, and J. Feist, Nat. Commun. **7**, 13841 (2016).

[38] J. Galego, F. J. Garcia-Vidal, and J. Feist, Phys. Rev. Lett. **119**, 136001 (2017).

[39] L. A. Martínez-Martínez, R. F. Ribeiro, J. Campos-González-Angulo, and J. Yuen-Zhou, ACS Photonics **5**, 167 (2018).

[40] T. W. Ebbesen, Acc. Chem. Res. **49**, 2403 (2016).

[41] J. Feist, J. Galego, and F. J. Garcia-Vidal, ACS Photonics **5**, 205 (2017).

[42] R. F. Ribeiro, L. A. Martínez-Martínez, M. Du, J. Campos-González-Angulo, and J. Yuen-Zhou, Chem. Sci. **9**, 6325 (2018).

[43] A. Nazir and D. P. S. McCutcheon, Journal of Physics: Condensed Matter **28**, 103002 (2016).

[44] D. Polak, R. Jayaprakash, T. P. Lyons, L. A. Martínez-Martínez, A. Leventis, K. J. Fallon, H. Coulthard, D. G. Bossanyi, K. Georgiou, A. J. Petty, II, J. Anthony, H. Bronstein, J. Yuen-Zhou, A. I. Tartakovskii, J. Clark, and A. J. Musser, Chem. Sci. **11**, 343 (2020).

[45] E. Eizner, L. A. Martínez-Martínez, J. Yuen-Zhou, and S. Kéna-Cohen, Science Advances **5** (2019), 10.1126/sciadv.aax4482, <https://advances.sciencemag.org/content/5/12/eaax4482.full.pdf>

[46] L. A. Martínez-Martínez, E. Eizner, S. Kéna-Cohen, and J. Yuen-Zhou, The Journal of Chemical Physics **151**, 054106 (2019), <https://doi.org/10.1063/1.5100192>.

[47] R. H. Dicke, Phys. Rev. **93**, 99 (1954).

[48] M. Gross and S. Haroche, Physics Reports **93**, 301 (1982).

[49] A. V. Andreev, V. I. Emel’yanov, and Y. A. Il’inskii, Soviet Physics Uspekhi **23**, 493 (1980).

[50] M. Tavis and F. W. Cummings, Phys. Rev. **170**, 379 (1968).

[51] M. O. Scully and M. S. Zubairy, *Quantum Optics* (Cambridge University Press, 1997).

[52] M. S. Skolnick, T. A. Fisher, and D. M. Whittaker, Semiconductor Science and Technology **13**, 645 (1998).

[53] E. Brion, L. H. Pedersen, and K. Mølmer, Journal of Physics A: Mathematical and Theoretical **40**, 1033 (2007).

[54] J. Keeling, “Light-matter interactions and quantum optics,” (2014).